C. R. Physique 3 (2002) 543–554

Solides, fluides : propriétés électroniques et optiques/*Solids, fluids: electronic and optical properties*
(Surfaces, interfaces, films/*Surfaces, interfaces, films*)

DOSSIER

PHOTONIQUE MOLECULAIRE : MATÉRIAUX, PHYSIQUE ET COMPOSANTS

MOLECULAR PHOTONICS: MATERIALS, PHYSICS AND DEVICES

Electro-optic polymer based devices and technology for optical telecommunication

Patrick Labbé [a,b]*, Ariela Donval [a], R. Hierle [a], Eric Toussaere [a], Joseph Zyss [a]

[a] **Laboratoire de photonique quantique et moléculaire, UMR-CNRS 8537, École normale supérieure de Cachan, 61, av. Du Président Wilson, 94235 Cachan, France**

[b] **Centre de recherche Motorola, Espace technologique de Saint-Aubin, 91193 Gif-sur-Yvette, France**

Accepted 1 March 2002

Note presented by Guy Laval.

Abstract Electro-optic polymer waveguide devices are very attractive for optical communication systems, because of their potentially simple and low-cost fabrication procedure. High bandwidth devices are enabled by the low dielectric constant of polymers with negligible dispersion from DC to optical frequencies. We first detail the modelization steps relating to the optical and electrical aspects of devices. We then outline the different steps of the fabrication process of electro-optic polymer based devices. By way of illustrating these considerations, we present some original realizations namely polarization insensitive modulators, switching devices using an asymetric X coupler and optic to RF converters based on difference frequency mixing. ***To cite this article: P. Labbé et al., C. R. Physique 3 (2002) 543–554.*** © 2002 Académie des sciences/Éditions scientifiques et médicales Elsevier SAS

electro-optic polymers / integrated optics / devices / optical telecommunication

Composants à base de polymères électro-optiques pour les télécommunications optiques

Résumé Les composants à base de polymères pour l'optique intégrée sont particulièrement intéressants pour les systèmes de télécommunications en particulier par leur procédé de fabrication simplifié et à bas coût. Leur grande bande passante résulte en partie de leur faible constante diélectrique ainsi que d'une dispersion très réduite depuis les signaux continus jusqu'aux fréquences optiques. Nous détaillons tout d'abord les étapes de modélisation concernant de façon conjointe les aspects optiques et électriques. Le procédé de fabrication de ces composants est exposé dans une seconde partie. Enfin, des résultats originaux seront présentés concernant un modulateur insensible à la polarisation, un commutateur intégrant une jonction en X asymétrique ainsi qu'un convertisseur optique hyperfréquence utilisant les propriétés non linéaires de génération de différence de fréquences. ***Pour citer cet article : P. Labbé et al., C. R. Physique 3 (2002) 543–554.*** © 2002 Académie des sciences/Éditions scientifiques et médicales Elsevier SAS

* Correspondence and reprints.
E-mail address: patrick.labbe@motorola.com (P. Labbé).

S1631-0705(02)01334-8/FLA

polymères électro-optiques / optique intégrée / composants / télécommunications optiques

1. Introduction

Over the last decade, optical telecommunication systems have been constantly expanding. Following their initial vocation towards long-haul transmission with national and inter-continental coverage exploiting the low absorption of silica-based optical fibers (< 0.2 dB/km), activities in the domain have gradually come to encompass local area networks. In order to face a constant increase of the demand in terms of data rates, various features of the optical and electrical equipment need to be continuously upgraded. At the same time, progress is being met and challenged by new problems, such as the periodical attenuation due to fiber dispersion at the high frequency modulation regime [1] (single side band modulation techniques) or the need of signal reshaping and amplification for inter-continental links (amplifier with Er-doped fiber). Thanks to these improvements, modulators are commercially available at 40 GHz and above and the data rate along a fiber link has exceeded a Tbit/s during year 2000 [2] which, in turn, set new problems.

Optical transmission requires encoding of the electrical signal onto the frequency carrier at variable frequency rates, depending on the application. For such a purpose, several key devices are involved in the link:

(i) an intensity modulator (Mach–Zehnder based [3] or electro-absorption modulator) acting as an electric-to-optic converter;
(ii) some routing devices (switch, MUX and deMUX); and
(iii) a photodiode acting as an optic to RF converter (MSM, PIN or PIN-guide photodiode).

Until the last decade, these functions were mainly sustained by $LiNbO_3$, AsGa, or InP based devices depending on the operating wavelength or the specific purpose. Since the end of the 1980s, a new generation of polymer-based devices has emerged and gradually matured. Initially investigated mainly for their high non-linear response, high bandwidth and low dielectric constant, they also became very attractive for their adaptability to different applications: low-loss polymers for passive waveguides [4], cross-linkable matrix to increase mechanical robustness of the device or highly effective molecules to enhance non-linear response [5]. Polymers offer interesting possibilities essentially deriving from their simpler fabrication route that will be outlined in the next section. At present, polymers allow for the development of new low-cost fibers and new electro-optic devices for modulation or switching coming close to actual system deployment. The latter applications will be detailed in the last section of this article.

2. Device modeling

Modeling of devices is prerequisite to their optimization and must account for two different aspects. Firstly, the optical behavior is related to the modal distribution of the waveguide taking into account its full 2D transverse optical geometry including the different optical index domains as well as the propagation of the signal along the device. Secondly, electrical modeling provides estimates of the poling field during the fabrication process as well as the matching of the electrical and optical fields pertaining to modulation.

2.1. Optical modeling

The optical mode profiles (Fig. 1(a)) are calculated taking into account the strong index contrast of polymer structures which can reach optical index differences up to 0.4 between two consecutive layers. Towards that aim, the software Alcor, developed by France Telecom R&D, allows one to calculate, via enhanced Galerkine algorithms, the electrical part of the optical wave and establish a transverse map of the different characteristic values. This study then makes possible the determination of the confinement for each

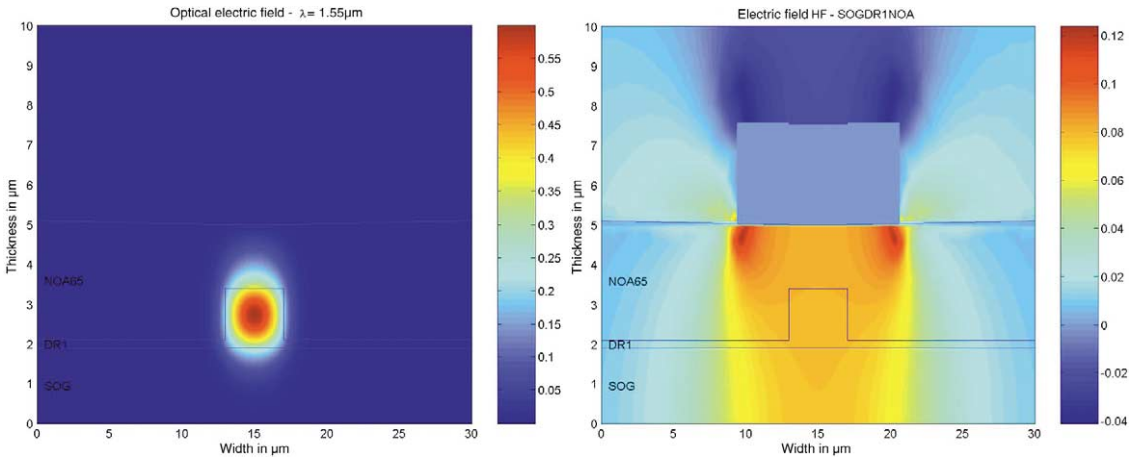

Figure 1. Optical (left) and electrical (right) mapping of a three-layers polymeric structure.

Figure 1. *Modélisation des modes optiques à gauche et électrique à droite d'une structure polymère tri-couche.*

mode and the prediction of possible scattering problems due to interface roughness. This essential phase helps to determine an effective benchmarking structure in order to guide subsequent clean room processing steps.

In a second calculation phase, the propagation of the wave is simulated by studying the coupling from one finite element to the next throughout the device. The coupling coefficient (noted c_{ij}) between the ith and jth mode of two consecutive elements (respectively named 0 and 1) in terms of the phase α and amplitude A were calculated according to [6]

$$A_{j1} = \sum_{i=0}^{m} c_{ij} A_{i0} \cos(\alpha_{i0} - \alpha_{j1}), \tag{1}$$

$$c_{ij} = \frac{2\sqrt{n_{i0}^{\text{eff}} n_{i1}^{\text{eff}}}}{n_{i0}^{\text{eff}} + n_{j1}^{\text{eff}}} \frac{n_{i0}^{\text{eff}} + n_{j1}^{\text{eff}}}{n_{i0}^{\text{eff}} + n_{i1}^{\text{eff}}} \frac{I_{i0,j1}}{\sqrt{I_{i0,i0} I_{j1,j1}}}, \tag{2}$$

$$\tan(\alpha_{j1}) = \sum_{i=0}^{m} c_{ij} A_{i0} \cos(\alpha_{i0}) \Big/ \sum_{i=0}^{m} c_{ij} A_{i0} \sin(\alpha_{i0}), \tag{3}$$

where $I_{i,j}$ is the overlap integral between the ith and jth mode. We are then able to predict the propagation along the full device extension.

2.2. Electrical modeling

The next and connected modeling step consists in mapping-out the electrical field distribution corresponding to a given potential applied on the command electrode (Fig. 1(b)). During the poling step, the effective intensity of the field needs to be transferred to the core polymer. This requirement is investigated by means of a finite dimension algorithm implemented under Matlab in order to solve the Laplace equation on a given mesh. Resistivity measurements of our different polymers provide the necessary data in order to simulate the waveguide structures.

To evaluate the RF mode profile of a microstrip line, it is possible to apply the previous method because the RF mode is obtained from an equation similar to the Laplace equation with the permitivity of the different polymers now replacing their resistivity.

3. Polymer processing steps for device fabrication

Polymers offer very broad possibilities in terms of synthesis based on a targeted molecular engineering approach. It is indeed possible to design and fabricate tailored molecules with prescribed absorption and emission spectra as well as their index of refraction and nonlinear properties. Polymers for optical waveguides are indeed chosen for: (i) their optical index eventually coming close to that of silica-based fibers in a range typically from 1.4 to 1.9; (ii) their mechanical qualities; and (iii) long term stability. One of the main expected advantages is the reduction of Fresnel losses so as to minimize the return signal in the link which reduces the quality of the transmission. It also enables easier and more robust fabrication steps while increasing the lifetime of the device.

3.1. Fabrication

The fabrication process of polymeric devices is derived from classical micro-electronic fabrication steps [7]: spin-coating deposition, UV photolithography and reactive ion etching have been adapted to polymer processing. Optical polymer waveguides are built up from successive layer depositions in order to set-up a 3-level guiding structure comprising the lower cladding polymer, the core polymer eventually endowed with electro-optic properties (depending on the application) and the upper cladding. The layers are defined according to the targeted geometry and their respective index to ensure the waveguiding confinement property and to prevent unexpected parasitic planar waveguide effects. In order to deposit the different layers, the successive spin-coating steps are advantageously replacing epitaxial deposition of semi-conductor layers which is heavily constrained by lattice matching requirements whereas polymer adhesion offers a very broad range of more flexible solutions. Spin coating consists in depositing the polymer in solution upon a substrate (semi-conductor wafer or silica plate) which is rotated at thousands of rounds per minute to yield an homogenous layer of 0.1 to 4 μm thickness, depending on the viscosity and volatility of the solvent. Moreover, the thickness range can be slightly tuned by the dilution of the prepared solution. The shape imprinted onto the guiding layer is obtained from classical reactive ion etching and UV photolithography: electrooptic polymers are quite similar in structure to photoresists, which makes oxygen plasma etching an efficient tool also in this context. An etching rate of the order of 0.1 μm per minute enables a good control of the etching depth. Nevertheless, comparable orders of magnitude for the etching rates of polymers and photoresists put a limitation on the etching depth in high resolution conditions. However, test patterns of 0.5 μm depth have been realized with a good quality.

In the case of active polymers, command electrodes are realized by sputtering upon the upper cladding without any overlayer. The top electrodes are delineated with standard photolithography and wet etching techniques with a potassium iodide (KI) solution at a concentration adapted to the rate processing. The fabrication process is summarized in Fig. 2 and a typical structure is presented in Fig. 3.

3.2. Orientation

In the case of active devices based on the electro-optic (linear Pockels) effect, breaking the centrosymmetry at the macroscopic level is a prerequisite condition. As the spin coating deposition does not favor any preferential orientation of the chromophores in the matrix, additional poling methods are needed to ensure this requirement. The most widely used technique is based on the dipole–field interaction and applies therefore preferably to molecules with a strong dipolar component. It consists in heating the polymer up to its glassy temperature making the molecule free to move according to different degrees of freedom. Applying a static electrical field to the structure via a needle to create a Corona field or via driving electrodes allows to statistically orient the molecules along the poling field direction. The centrosymmetry of the medium is then broken for reasons similar to that applying to the Electric Field Induced Second Harmonic (EFISH) methods in solution [8]. Cooling the system down to room temperature subsequently freezes the molecules in their polar statistical order. The induced order is preserved at operating temperature after the poling field is cut as a result of chemical engineering efforts to limit relaxation effects [9]. Such an orientation is relying

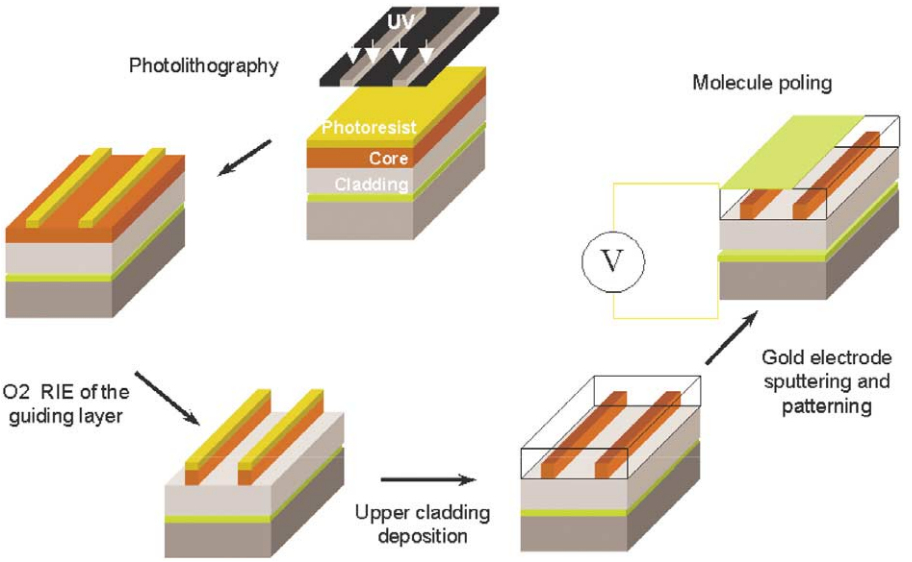

Figure 2. Different steps involved in the fabrication process.

Figure 2. *Différentes étapes du procédé de fabrication.*

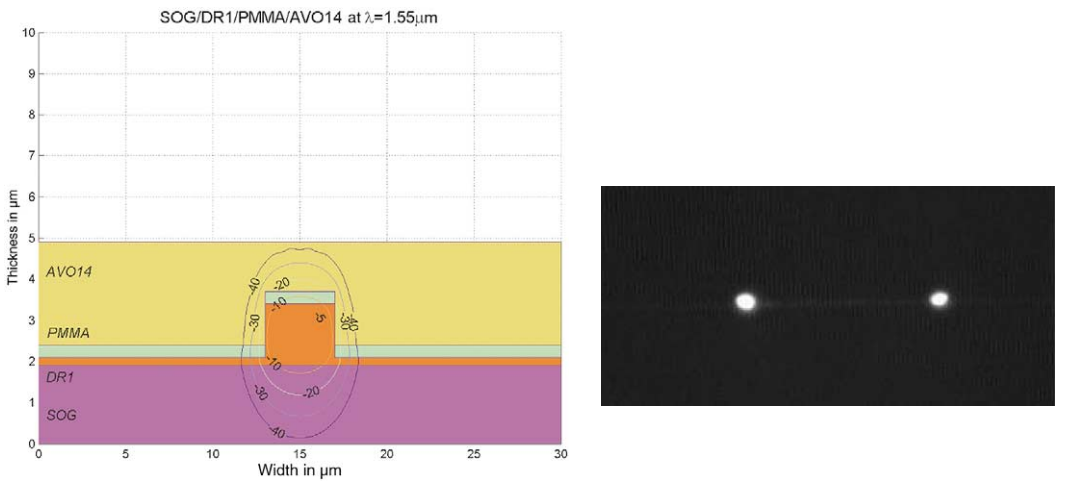

Figure 3. Mode profile of a guiding structure of SOG (Spin On Glass) / PMMA-DR1 (PolyMethylMetAcrylate-Disperse Red 1) / PMMA / AVO14 (Anne-Valérie Ochs 14) (left). Output of a 1 to 2 junction observed with an IR camera. The two arms are 250 μm apart (right).

Figure 3. *A gauche : structure de guide SOG/PMMA-DR1/PMMA/AVO14. A droite : sortie observée par une caméra infrarouge d'une jonction* 1 *vers* 2 *dont les bras sont distants de* 250 μm.

on statistical effects the stability of which depends on the interaction between active and passive molecules in the polymer. Another increasingly important class of methods consists in interfering two laser beams to imprint a controlled temporal pattern with dipolar or octupolar symmetry features, depending on the polarization of the writing beam and the symmetry of the chromophores [10]. It may also be advantageous to combine electrical and optical poling to the so-called photo-assisted poling technique [11,12].

The quality of the poling process as well as the efficiency of the end goal electrooptic effect of interest is reflected in the value of the r_{33} coefficient of the electrooptic tensor. The half-wave quenching voltage V_π of a phase modulator can be inferred from r_{33} by

$$r_{33} = \frac{3\pi\lambda}{2V_\pi L n^3}, \tag{4}$$

L is the electrode length, n the linear index, λ the wavelength of operation. However, inferring r_{33} from V_π requires that a complete device be processed which may be inadequate for large scale screening of materials at a preliminary selection stage. A possibly more appropriate method consists then in inferring r_{33} from the second harmonic generation response of the bulk material which only requires thin layer deposition and electric field poling of the polymer [13]. A quantum two-level model of the molecular quadratic non linearities leads to a relation between the second harmonic coefficient $\chi^{(2)}_{zzz}(-2\omega;\omega,\omega)$ and the electro-optic coefficient $r_{33}(-\omega;\omega,0)$, namely:

$$r_{33}(-\omega;\omega,0) = -\frac{2}{n_\omega^4}\frac{f^0}{f^{2\omega}}\frac{(3\omega_0^2-\omega^2)(\omega_0^2-4\omega^2)}{3\omega_0^2(\omega_0^2-\omega^2)}\chi^{(2)}_{zzz}(-2\omega;\omega,\omega), \tag{5}$$

where ω is the fundamental laser frequency, ω_0 is the absorption peak frequency of the polymer, n_ω the refractive index at frequency ω; $f^{2\omega}$ and f^0 are Lorenz–Lorentz and Onsager local field factors, respectively, given by

$$f^\omega = \frac{n_\omega^2+2}{3}, \qquad f^0 = \frac{\varepsilon(0)(n_\infty^2+2)}{2\varepsilon(0)+n_\infty^2}, \tag{6}$$

where $\varepsilon(0)\sim 4.5$ and $\chi^{(2)}_{zzz}(-2\omega;\omega,\omega) = 2d_{33}$. Experimental d_{33} and r_{33} values are in good agreement with this model for cross-linked polymers such as PMMA-DR1 and Magly [CNET patent n°9310572] at 30% mass concentration.

To increase the lifetime of devices, considerable efforts have been invested over the last decades to ensure that the links between chromophores and the matrix are strengthened while leaving enough flexibility to allow for poling mobility. From a doped polymer where chromophores are diluted into a host matrix (Fig. 4), interest has moved to side-chain polymers [14] where chromophores are tethered via a covalent bond to the hosting matrix and then finally to cross-linkable molecules [15]. In this case, a second bond is activated after the orientation process thus freezing final orientation in a locked structure at an affordable expense to the pre-linked polar order. Finally, recent work aims at increasing the rigidity of the host matrix in order to prevent the potential rotations between monomers by use of high glass transition temperature (T_g) polymers [16].

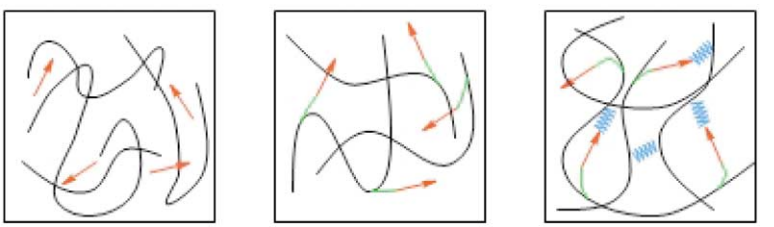

Figure 4. Insertion method of chromophores into an amorphous matrix. From left to right are guest–host, tethered and crosslinkable systems.

Figure 4. *Méthodes d'insertion de molécules dans une matrice amorphe. De gauche à droite sont représentés des systèmes dopés, substitués et réticulés.*

Moreover, polymeric devices present the advantage of an adjustable symmetry in order to match the needs of dedicated applications: push–pull orientation to decrease by half the quenching tension and polarization insensibility for telecom application.

4. Illustrative electrooptic devices

Rather then being exhaustive in view of the considerable amount of results in the field, we intend in the following to illustrate the specificity and advantages of polymer-based devices by referring to several original applications.

4.1. Classical modulator based on the Mach–Zehnder interferometer

The principle of a Mach–Zehnder interferometer consists in beating two beams, one of which previously dephased by propagation along a waveguide submitted to an electrooptic perturbation. A set of electrodes surrounding one waveguiding arm allows for the application of a voltage and subsequent dynamical control of the index of the waveguide [3]. These electrodes can be engineered in sandwich or coplanar configuration, depending on the coefficient of the electrooptic tensor which is of interest towards a given application. Considering a fixed propagation length under electrode, the induced phase mismatch depends on both magnitudes of the electrooptic coefficient and of the applied voltage. Bandwidth, insertion losses and quenching voltage are the main features which characterize such generic device. A wealth of results can be found in the literature with the demonstration of record breaking performances: a 110 GHz bandwidth modulator [17] and a 0.8 V quenching voltage modulator have been evidenced [18]. Such features are partly due to the configurations of electrodes but they also emphasize the advantages of new polymer materials in terms of bandwidth and electro-optic response. This family of device opens the way to various specific applications suited to special needs.

4.2. Polarization insensitive modulators

Most electrooptic devices do not present similar responses along the two main polarization axes. Such an imbalanced response leads to a decrease of modulation efficiency or to additional losses if the signal is propagating along a polarization maintaining fiber. In order to solve this problem, different approaches have been proposed which build up on intrinsic advantages of polymers due to their flexible structure.

The first one consists in designing a dedicated set of electrodes allowing for the application of a control field simultaneously along the horizontal and vertical axes. Such a device has been made using substituted PMMA-DR1 as the core polymer and NOA61 and 65 optical adhesives as the cladding polymers (Fig. 5).

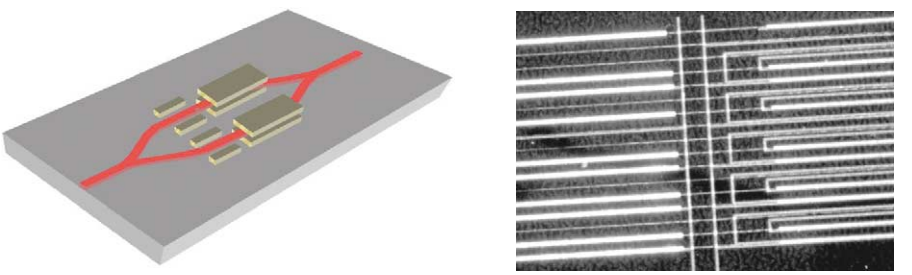

Figure 5. Polarization insensitive modulator with a dedicated sequence of in-place lateral and superimposed vertical electrodes (left). Detailed of the electrodes observed through a microscope objective × 20 (right).

Figure 5. *Modulateur insensible à la polarisation employant deux jeux consécutifs d'électrodes sur chaque bras de l'interféromètre, en géométrie parallèle dans le plan du substrat et superposé* (*schéma de gauche*). *Détail des électrodes observé au microscope* × 20 (*photo de droite*).

Still unoptimized extinction tensions of 32 and 80 V have been measured along the vertical and horizontal polarization axes respectively [19]. Moreover, high stability of the device has been observed at 80 °C over months. Ongoing studies are currently aiming at taking advantage of all-optical orientation techniques which allow for the control of the molecular orientation by the specific configuration of the ω and 2ω writing beams configuration [20].

4.3. Electro-optic switch

Optical switches are one of the main cornerstones of current telecommunication systems, allowing the routing of information through optical fiber networks to an adequate intermediary or final destination. Therefore the development of such devices is of fundamental importance and many solutions have been reported in the literature based on different design principles leading to a broad range of switching times and component technologies. The first switches based on an asymmetrical junction were implemented based on Ti:$LiNbO_3$ technology in the 1970s with the most recent applications to circulators exhibiting driving voltages from 15 to 45 V depending on the *TE* or *TM* mode configuration [21]. Based on the same principle, a circulator designed on GaAs present driving commands of 12.5 V for 5 mm long electrodes and a bandwidth higher than 1.6 GHz [22].

The first polymer-based demonstrations rely on the thermo-optical phenomena, which restricts the bandwidth to 50 Hz [23]. Electrooptic polymers potentially allowing for high frequency operation [17] as well as low driving voltage [24] have been implemented in 2×2 circulators [25] and more recently in a modulator with a directional coupler at the output, with performances comparable to those of currently available devices [26]. We have conceived, fabricated and tested an electrooptic polymer based 1×2 switch made of an amplitude modulator combined with an asymmetric X junction at its output. The device exploits modal evolution in order to circumvent critically precise control of the refractive index and of the waveguide dimensions.

The operation of the device is based on the modal behavior of an X-asymmetric junction consisting of two junctions placed head-digs, the outgoing one with arms of different widths. Modal analysis of such a structure exhibits two distinct behaviors [27]. The symmetrical side is able to sustain two modes, the first being symmetric while the second one is antisymmetric, thus leading to a balanced distribution of the energy. The asymmetrical part can also sustain the two modes but the main portion of the energy is then concentrated in one of the two arms, the first symmetric mode confined within the broader arm while the narrower one sustains the second asymmetric mode [6]. Since a given mode will be best coupled to that with the closest propagation constant, the symmetrical mode preferentially excites the broadest arm while the antisymmetric mode conversely excites the narrowest one. The main parameter that enables one to control the efficiency of the transition is the branching angle between waveguides. The adiabatic character of the transition is ensured by angles less than 1°. Smaller angles would lengthen the transition resulting into longer devices and excess losses. Thus, it is possible to choose the output arm on the asymmetrical side by controlling the relative phase between the two arms at the entrance of the symmetrical side (see Fig. 6).

To this end, we used a symmetrical 1×2 junction, which allow to split the signal into two parts with identical phase and intensity. Then, the EO polymer enables to obtain a controlled phase mismatch between the two arms via a voltage applied to independent electrodes embedding the waveguide, according to [28]:

$$\Delta\varphi^{TM} = \frac{\pi}{\lambda}\frac{n_e^4}{n_{\text{eff}}} r_{33}\Gamma L\frac{V}{d} \tag{7}$$

where λ is the optical wavelength, n_{eff} is the effective *TM* index of the complete structure, n_e is the extraordinary index, d is the distance between the electrodes, L the electrode length and Γ is the overlap integral between the applied electrical field and the optical field. Finally, the output arm is directly controlled by the electrical signal applied on the electrode leading to a device with switching as well as a modulating potential and two complementary outputs.

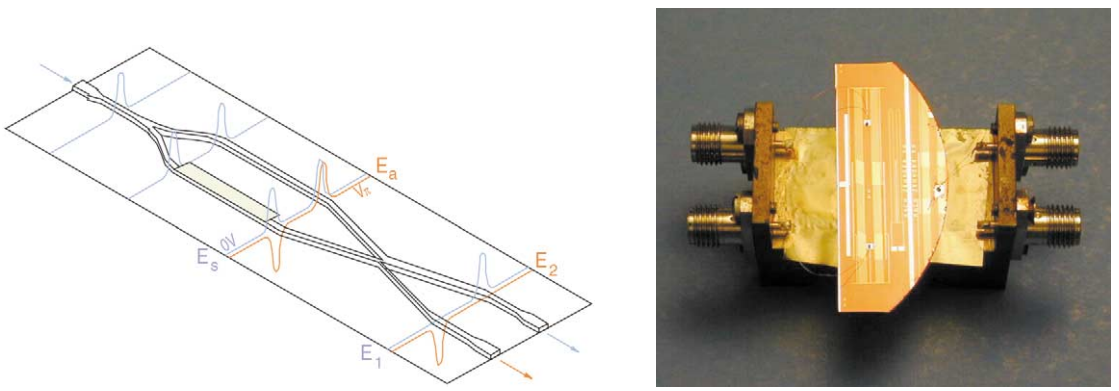

Figure 6. Operating principle of the electro-optic switch including an asymmetric X junction as the output coupler (left). Picture of the final device packaged in a SMA connectorized mount.

Figure 6. *Principe de fonctionnement du commutateur électro-optique incluant une jonction en X asymétrique en sortie. Photo du composant final mis en boîtier avec connecteurs SMA.*

Such a device has been realized with substituted PMMA-DR1 as core polymer and SOG and NOA65 as cladding polymers. An electrooptic coefficient of the order of 15 pm/V has been measured following a classical orientation scheme using modulation electrodes. It has been shown that the extinction ratio between the two outputs can be tuned by controlling the relative effective index difference of the two arms (the different sizes of the four arms of the coupler being fixed).

4.4. Optic to RF converter

Optical rectification is a quadratic nonlinear effect resulting from the beating of two beams of identical wavelength leading to a static interaction term and the related generation of a static polarization field.

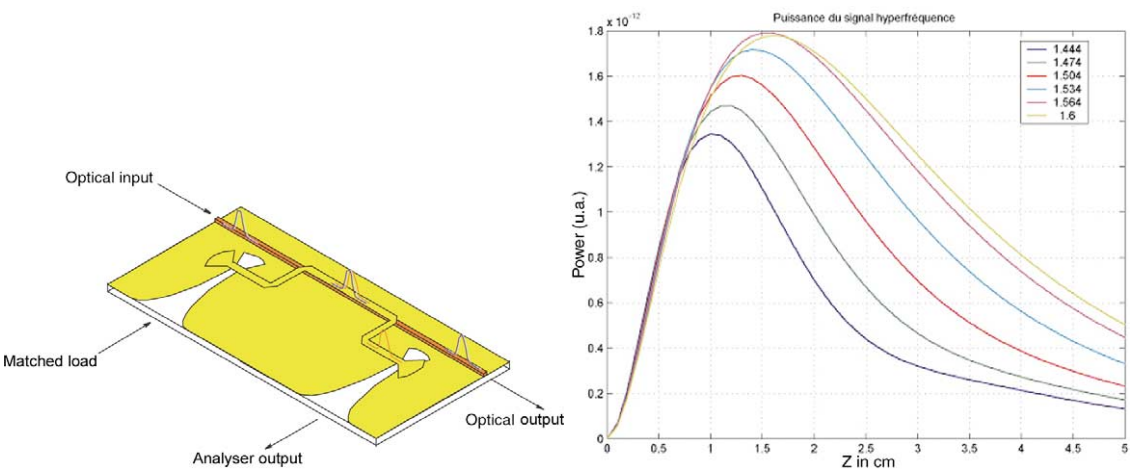

Figure 7. Operating principle of the optic to RF converter (left). Plot of the generated signal intensity along the propagation axis for different phase matching conditions (right).

Figure 7. *Principe de fonctionnement du convertisseur optique hyperfréquence* (*à gauche*). *Évolution du signal généré au cours de la propagation pour différentes conditions d'accord de phase* (*à droite*).

By way of extension, we will associate this phenomenon with the interaction of two optical waves with frequencies close enough to generate a radio frequency electrical signal at a lower frequency as compared to the optical domain (i.e. up to the THz range). Some studies of THz signal generation by optics have already been reported during the last two decades in $LiNbO_3$ crystals [29] and more recently in DAST (dimethyl amino 4-N-methyl stilbazolium tosylate) organic crystals [30]. Optical frequency mixing in AlGaAs waveguides has been performed in the X-band ($\sim$ 10 GHz) in order to provide a tunable RF source [31]. Our aim is to demonstrate the feasibility of similar devices using electrooptic polymer operating in the 60 GHz emission domain. To realize the conversion functionality, it is proposed to embed an optical ridge waveguide and a microstrip line so that the three waves can interact throughout the propagation length in a non centro-symmetric poled polymer as shown in Fig. 7.

Optical rectification can be modeled by adapting Manley–Rowe equations to waveguiding configurations. The guided wave case can be inferred from the bulk configuration by further introduction of field modal decomposition of the field and by introduction of a η coefficient reflecting the overlap between the optical and electrical fields. The evolution of the reduced amplitudes of the interfering fields, A_1 at frequency ω, A_2 at frequency Ω and A_3 at frequency $\omega + \Omega$ are then governed by the following equations:

$$\begin{cases} \dfrac{\mathrm{d}A_1}{\mathrm{d}z} = j\tilde{\eta}_1 \chi^{\mathrm{eff}} A_3 A_2^* \,\mathrm{e}^{-j\Delta k z} & \tilde{\eta}_1 = \eta_1 \dfrac{\langle E_3 E_2^* \mid E_1 \rangle}{\langle E_1 \mid E_1 \rangle}, \\ \dfrac{\mathrm{d}A_2}{\mathrm{d}z} = j\tilde{\eta}_2 \chi^{\mathrm{eff}} A_3 A_1^* \,\mathrm{e}^{-j\Delta k z} \quad \text{with} & \tilde{\eta}_2 = \eta_2 \dfrac{\langle E_3 E_2^* \mid E_2 \rangle}{\langle E_2 \mid E_2 \rangle}, \\ \dfrac{\mathrm{d}A_3}{\mathrm{d}z} = j\tilde{\eta}_3 \chi^{\mathrm{eff}} A_1 A_2 \,\mathrm{e}^{j\Delta k z} & \tilde{\eta}_3 = \eta_3 \dfrac{\langle E_1 E_2^* \mid E_3 \rangle}{\langle E_3 \mid E_3 \rangle}, \end{cases} \tag{8}$$

where E_i are the corresponding 2D field map.

It can be shown that the device will be all the more efficient if the targeted emission frequency is high and the optical input signals are intense. Concerning the interaction length, a compromise between the conflicting requirements of difference frequency generation versus absorption in the different materials leads to an optimal length. The results obtained for the modeling of such a dual waveguide with a SOG/DR1/NOA65 polymeric multi-layer, 1 mW of input optical power at a wavelength of 1.55 µm and a microstrip line of 50 Ω impedance is illustrated in Fig. 7.

In the case of RF generation by nonlinear optical mixing, the phase matching condition corresponds to the matching of the optical group velocity and the millimeter wave phase velocity as shown in Eq. (8):

$$\Delta k = 0 \quad \Leftrightarrow \quad \frac{\mathrm{d}k_\omega}{\mathrm{d}\omega} = \frac{k_\Omega}{\Omega} \quad \Leftrightarrow \quad v_{\mathrm{gr}}^{\mathrm{opt}} = v_{\mathrm{ph}}^{\mathrm{RF}}. \tag{9}$$

Fulfilling the phase matching condition is of critical importance to enhance the efficiency of the radiofrequency generation process so that it is crucial to determine and tune precisely the effective index of the different waves. If the RF index is higher than the optical index, the signal will be scattered by Cherenkov effect. In this case, the generated power is proportional to the frequency of the generated wave and not to the square of the frequency, the latter regime prevailing when the phase matching condition is fulfilled along the propagation pathway. When the phase matching condition is met, the generated wave is guided in the microstrip line. The RF index of polymers can be inferred from the effective dielectric constant of a reference coplanar waveguide and estimated to lie around 1.75 at 40 GHz [32]. The RF index has also been determined for the bulk material using the measured absorption of a self-supported PMMA-DR1 sample by Fourier transform spectrometry and subsequent Kramers–Kroenig analysis. Moreover, a preliminary THz generation experiment has emphasized that the polymer index is roughly constant between 5 and 35 THz. As the effective index of the optical and RF waveguides are fixed by their size, it is then possible to tune the optical rectification phase matching conditions.

5. Conclusions

Over the last decade, electrooptic polymer devices have been maturing fast all the way from early orientationnal stabilization studies to the ripening technologies for telecommunication applications standing on the verge of industrially developments. However, they still face some limitations in terms of propagation and insertion losses. Such drawbacks should be overcome through the upcoming industrial development phase. One main problem concerning the availability of the different polymers will have to be solved. In order to implement and calibrate a complete and robust fabrication process, it is indeed necessary to access different materials in sufficient quantities, a need which is likely to further trigger industrial undertakings.

The prospects in this field are large enough so as to justify further extension of the current academic effort into industrial ventures. The flexibility of the polymer synthesis allows to envision further functionnalization such as towards infrared luminescence which should enable the development of multifunctional polymer based modules with combined propagative, electrooptic and amplifying properties. Moreover, integration techniques between polymeric-based devices and silica-based devices may help solving the insertion loss problem by gradual adaptation of the mode shape.

Another boosting factor is likely to play an increasing role in the future. Whereas the technology steps displayed in Fig. 2 exemplify the obvious benefits of adapting preexisting semiconductor optoelectronics technology to the new field of polymers, the advent of specific polymer based technologies taking advantage of the virtues of polymers per se is gradually taking-over. Indeed, soft lithography, ink-jet printing, moulding and stamping, the use of flexible substrates as well as other approaches remaining to be discovered will renew the potential of polymer based photonics and open-up actual industrial possibilities in terms of low cost and high volume production in-keeping with the predictable demands for increased intelligence and higher data stream to meet the demands of domestic as well as professional end-users.

Acknowledgements. Part of this work (optic to RF converter) has been performed within a partnership between the École normale supérieure based in Cachan and the Centre de recherche Motorola based in Gif-sur-Yvette which is gratefully acknowledged.

References

[1] U. Gliese, S. Norskov, T.N. Nielsen, Chromatic dispersion in fiber-optic microwave and millimeter wave links, IEEE Trans. Microwave Theory Techn. MTT-40 (10) (1996) 1716–1724.
[2] L. du Mouza et al., 1.28 Tbit/s (32 × 40 Gbit) WDM transmission over 2400 km of Teralight/sup TM/Reverse Teralight fibres using distributed all Raman amplification, Electron. Lett. 37 (21) (2001) 1300–1302.
[3] R.C. Alferness, Waveguide electro-optic modulators, IEEE Trans. Microwave Theory Techn. MTT-30 (8) (1982) 1121–1137.
[4] R. Yoshimura, M. Hikita, S. Tomaru, S. Imamura, Low-loss polymeric optical waveguides fabricated with deuterated polyfluoromethacrylate, J. Lightwave Technol. 16 (6) (1998) 1030–1037.
[5] M. Ahleim, M. Barzoukas, P. Bedworth, M. Blanchard-Desce, A. Fort, Z.Y. Hu, S.R. Marder, J.W. Perry, C. Runser, M. Staehelin, B. Zysset, Chromophores with strong heterocyclic acceptors: a poled polymer with a large electro-optic coefficient, Science 271 (1996) 335–337.
[6] W. Burns, A. Milton, Mode conversion in planar-dielectric separating waveguides, IEEE J. Quantum Electron. QE-11 (1975) 32–39.
[7] R. Levenson, J. Liang, C. Rossier, R. Hierle, E. Toussaere, N. Bouadma, J. Zyss, Advances in organic polymer-based optoelectronics, in: Polymers for Second-Order Nonlinear Optics, Chapter 32, American Chemical Society, 1995, pp. 437–455.
[8] J.L. Oudar, Optical nonlinearities of conjugated molecules. Stilbene derivatives and highly polar aromatic compounds, J. Chem. Phys. 67 (2) (1977) 446–457.
[9] S. Yilmaz, W. Wirges, S. Bauer-Gogonea, S. Bauer, R. Gerhard-Multhaupt, F. Michelotti, E. Toussaere, R. Levenson, J. Liang, J. Zyss, Dielectric, pyroelectric, and electro-optic monitoring of the cross-linking process and photoinduced poling of Red Acid Magly, Appl. Phys. Lett. 70 (1997) 568–570.
[10] S. Brasselet, J. Zyss, Control of the polarization dependence of optically poled nonlinear polymer films, Opt. Lett. 22 (19) (1997) 1464–1466.

[11] Z. Sekkat, M. Dumont, Photoassisted poling azo dye doped polymeric films at room temperature, Appl. Phys. B 54 (5) (1992) 486–489.
[12] M. Dumont, A general model for optically induced molecular order in amorphousmaterials, via photoisomerisation, Nonlinear Opt. 9 (1995) 327–338.
[13] R. Levenson, J. Zyss, Polymer based optoelectronics: from molecular nonlinear optics to device technology, in: M. Quillec (Ed.), Materials for Optoelectronics, Kluwer, Boston, 1996.
[14] R. Levenson, J. Liang, E. Toussaere, N. Bouadma, A. Carenco, J. Zyss, G. Froyer, M. Guilbert, Y. Pelous, D. Bosc, Polymeric waveguides for electrooptic applications: material, characterization and device demonstration, Nonlinear Opt. 4 (1993) 233–243.
[15] J. Liang, R. Levenson, C. Rossier, E. Toussaere, J. Zyss, A. Rousseau, B. Boutevin, F. Foll, D. Bosc, Thermally stable cross-linked polymers for electro-optic applications, J. Phys. III 4 (12) (1994) 2441–2450.
[16] L. Bes, A. Rousseau, B. Boutevin, R. Mercier, B. Sillion, E. Toussaere, Synthesis and characterization of aromatic polyimides bearing nonlinear optical chromophores, High Perform. Polym. 12 (2000) 169–176.
[17] D. Chen, H.R. Fetterman, A. Chen, W.H. Steier, L.R. Dalton, W. Wang, Y. Shi, Demonstration of 110 GHz electro-optic polymer modulators, Appl. Phys. Lett. 70 (25) (1997) 3335–3337.
[18] Y. Shi, W. Lin, D.J. Olson, J.H. Bechtel, H. Zhang, W.H. Steier, C. Zhang, L.R. Dalton, Electro-optic polymer modulators with 0.8 V half-wave voltage, Appl. Phys. Lett. 77 (1) (2000) 1–3.
[19] A. Donval, E. Toussaere, R. Hierle, J. Zyss, New polarization insensitive electrooptic polymer amplitude modulator designed for integrated optic, J. Appl. Phys. 87 (7) (2000) 3258–3262.
[20] A. Donval, E. Toussaere, S. Brasselet, J. Zyss, Comparative assessment of electrical, photoassisted and all optical in-plane poling of polymer based electrooptic modulators, Opt. Mater. (Amsterdam) 12 (2–3) (1999) 215–219.
[21] Y. Silberberg, P. Perlmutter, J.E. Baran, Digital optical switch, Appl. Phys. Lett. 16 (19) (1987) 1230–1232.
[22] H. Feng, X. Li, Z. Yang, M. Wang, 2×2 GaAs asymetyric Mach–Zehnder interferometer switch, Appl. Phys. Lett. 60 (23) (1992) 2843–2845.
[23] M.-C. Oh, H.-J. Lee, M.-H. Lee, J.-H. Ahn, S. Han, Asymetric X-junction thermooptic switches based on fluorinated polymer waveguides, IEEE Photon. Technol. Lett. 10 (6) (1998) 813–815.
[24] A. Chen, V. Chuyanov, S. Garner, H. Zhang, W.H. Steier, Low V_π electro-optic modulator with a high $\mu\beta$ chromophore and a constant-bias field, Opt. Lett. 23 (6) (1998) 478–480.
[25] W.-Y. Hwang, M.-C. Oh, H.-M. Lee, H. Park, J.-J. Kim, Polymeric 2×2 electro-optic switch consisting of asymetric Y junctions and Mach–Zenhder interferometer, IEEE Photon. Technol. Lett. 9 (6) (1997) 761–763.
[26] D. An, Z. Shi, L. Sun, J. Taboada, Q. Zhou, X. Lu, R. Chen, S. Tang, H. Zhang, W. Steier, A. Ren, L. Dalton, Polymeric electro-optic modulator based on 1×2 Y-fed directional coupler, Appl. Phys. Lett. 76 (15) (2000) 1972–1974.
[27] D. Smith, J. Baran, J. Jackel, R. Wagner, R. Welter, A mode-evolution-type integrated-optical beam combiner for coherent receivers, IEEE Photon. Technol. Lett. 3 (4) (1991) 339–341.
[28] A.V. Ochs, A. Rousseau, B. Boutevin, E. Toussaere, A. Donval, R. Hierle, J. Zyss, Fabrication of low refractive index low loss fluorinated self-cross linking polymer waveguides for optical devices, in: Proc. 7th International Plastic Optical Fibres Conference, Berlin, 1998, pp. 316–323.
[29] L. Xu, X.-C. Zhang, D.H. Auston, Terahertz beam generation by femtosecond optical pulses in electro-optic materials, Appl. Phys. Lett. 61 (15) (1992) 1784–1786.
[30] X.-C. Zhang, X. Ma, Y. Jin, T.-M. Lu, E. Boden, P. Phelps, K. Stewart, C. Yakymyshyn, Terahertz optical rectification from a nonlinear organic crystal, Appl. Phys. Lett. 61 (26) (1992) 3080–3082.
[31] E. Frlan, S. Janz, F. Chatenoud, R. Normandin, M.G. Stubs, J.S. Wight, Generation of tunable, CW, microwave radiation in X-band by difference–frequency mixing, Electron. Lett. 30 (7) (1994) 595–597.
[32] J.-F. Larchanché, PhD thesis, USTL, 2001.